EPIGENETICS

Menin "reads" H3K79me2 mark in a nucleosomal context

Jianwei Lin[1]†, Yiping Wu[1]†, Gaofei Tian[1]†, Daqi Yu[2]†, Eunjeong Yang[4,5], Wai Hei Lam[6], Zheng Liu[1], Yihang Jing[3], Shangyu Dang[2], Xiucong Bao[4]*, Jason Wing Hon Wong[4,5]*, Yuanliang Zhai[6]*, Xiang David Li[1,3]*

Methylation of histone H3 lysine-79 (H3K79) is an epigenetic mark for gene regulation in development, cellular differentiation, and disease progression. However, how this histone mark is translated into downstream effects remains poorly understood owing to a lack of knowledge about its readers. We developed a nucleosome-based photoaffinity probe to capture proteins that recognize H3K79 dimethylation (H3K79me2) in a nucleosomal context. In combination with a quantitative proteomics approach, this probe identified menin as a H3K79me2 reader. A cryo–electron microscopy structure of menin bound to an H3K79me2 nucleosome revealed that menin engages with the nucleosome using its fingers and palm domains and recognizes the methylation mark through a π-cation interaction. In cells, menin is selectively associated with H3K79me2 on chromatin, particularly in gene bodies.

Methylation of lysine at various sites on histones regulates gene activation or repression, depending on which residues are modified and the degree of methylation (i.e., mono-, di-, or trimethylation) (*1*, *2*). Effector (or "reader") proteins are key players that recognize histone methylation and translate this information into downstream gene regulation events to control gene expression (*3*). So far, readers of almost all histone methylation marks have been identified except for methylation at histone H3 lysine 79 (H3K79). Although several "royal family" modules containing proteins have been implicated to interact with this mark, robust evidence for the recognition is lacking (*4*–*7*). In mammals, DOT1L is the methyltransferase that methylates H3K79 (mono-, di-, and trimethylation) (*8*, *9*). The DOT1L-mediated H3K79 methylation is enriched at actively transcribed genes and is involved in the regulation of transcriptional elongation, DNA damage repair, and cell cycle progression (*10*–*14*). In higher eukaryotes, the H3K79 methylation level is exquisitely controlled during embryonic development and hematopoiesis (*15*). Perturbation of H3K79 methylation in mouse embryo leads to cardiovascular defects and anemia (*16*). Aberrant hypermethylation of H3K79 was found to drive leukemogenesis in mixed lineage leukemia (MLL) (*17*). Despite the important roles of H3K79 methylation, understanding of how this histone mark is translated downstream to regulate these processes is hindered by a lack of knowledge about the readers of H3K79 methylation.

[1]Department of Chemistry, University of Hong Kong, Hong Kong SAR, China. [2]Division of Life Science, Hong Kong University of Science and Technology, Hong Kong SAR, China. [3]Greater Bay Biomedical InnoCenter, Shenzhen Bay Laboratory, Shenzhen, China. [4]School of Biomedical Sciences, University of Hong Kong, Hong Kong SAR, China. [5]Centre for Oncology and Immunology, Hong Kong Science Park, Hong Kong SAR, China. [6]School of Biological Sciences, University of Hong Kong, Hong Kong SAR, China.
*Corresponding author. Email: xiangli@hku.hk (X.D.L.); zhai@hku.hk (Y.Z.); jwhwong@hku.hk (J.W.H.W.); baoxc@hku.hk (X.B.)
†These authors contributed equally to this work.

Design and synthesis of photocrosslinkable nucleosomes with H3K79me2 mark

Identification of H3K79 methylation readers is challenging because the posttranslational modification (PTM)–mediated protein-protein interactions (PPIs) can be weak and transient. Recognition of H3K79 and its methylation is dependent on nucleosome context, because this residue is in the core region of the nucleosome within the well-defined quaternary structure. Indeed, DOT1L methylates H3K79 only in an intact nucleosome but not in H3 peptides or proteins (*8*). Therefore, a peptide-based biochemical "pull-down" may not be suitable. We thus designed a multifunctional synthetic nucleosome (probe N1) that carries a site-specific dimethylation on H3K79 at a stoichiometric level. The probe also consists of a cleavable photoaffinity handle containing a photoreactive group (i.e., diazirine) that can convert noncovalent weak interactions into irreversible covalent linkages upon ultraviolet (UV) irradiation, a biorthogonal handle (i.e., alkyne) that facilitates the isolation of cross-linked proteins, and a disulfide linkage that allows the release of cross-linked peptides for mass spectrometry (MS) analysis (Fig. 1, A and B). To ensure photocrosslinking efficiency and specificity, this trifunctional handle was placed at H3D81 position. This location is close to H3K79 and less likely to interfere with the histone-histone or histone-DNA interactions within the nucleosome, according to the crystal structure of the nucleosome (*18*) (fig. S1A).

To prepare probe N1, we first performed a multistep semi-synthesis to assemble *Xaenopus laevis* histone H3K79me2 (D81ADdis-Cys, C110A) (probe H1) through expressed protein ligation (*19*) (Fig. 1C). The N-terminal fragment (F1, residues 1 to 74) was produced recombinantly as an intein fusion to yield an α-thioester at its C-terminal residue, whereas the central segment containing K79me2 (F2, residues 75 to 80, A75C) was synthesized through Fmoc solid-phase peptide synthesis as an acyl hydrazide. The C-terminal fragment (F3, residues 81 to 135, D81C, C110A) was prepared recombinantly as a SUMO fusion, which was cleaved by Ulp1 to expose the N-terminal cysteine. The three fragments were joined by native chemical ligation (NCL) (*20*) in an N-to-C manner. After the first ligation, desulfurization yielded a new N-terminal fragment containing K79me2 (F1-2, residues 1 to 80), leaving the inert acyl hydrazide unaffected. Subsequent activation of the C-terminal acyl hydrazide by $NaNO_2$ oxidation and 4-mercaptophenylacetic acid (MPAA) thiolysis generated a new α-thioester for the second NCL to produce H3K79me2 (D81C, C110A) (fig. S1B). Taking advantage of the ligation "scar," in which the cysteine at residue 81 is the only cysteine in the ligation product, we installed the trifunctional handle at this position through an asymmetric disulfide exchange reaction with a 5-nitropyridyl-2-sulfenyl (Npys)–activated diazirino alkynyl hetero disulfide (Npys-Dzyne) to produce the desired product, H3K79me2 (D81ADdis-Cys, C110A) (probe H1). The identity of the product and the site-specific incorporation of the dimethyl lysine together with the trifunctional handle were confirmed by liquid chromatography–tandem mass spectrometry (LC-MS/MS) (Fig. 1, D and E). As a control protein probe, unmodified histone H3 (D81C, C110A) was expressed and purified from bacteria, followed by functionalization with Npys-Dzyne (fig. S1, C and D). Using a similar strategy, we also prepared H3K79me2 (C110A) without photocrosslinker (fig. S1, E and F). The synthesized dimethylated and unmodified H3 protein probes were then incorporated into mononucleosomes to generate probes N1 and N1c, respectively (Fig. 1, A and F).

Identification of menin as an H3K79me2-dependent nucleosome binder

We performed a standard cross-linking–assisted and SILAC-based protein identification (CLASPI) (*21*) experiment using probes N1 and N1c in both a "forward" and "reverse" manner. Proteins that preferentially bound to the K79-methylated nucleosome (probe N1) over the unmodified nucleosome (probe N1c) should have a higher SILAC H/L (heavy/light) ratio in the forward setting and a higher L/H ratio in the reverse setting (Fig. 2A). Most captured proteins in the CLASPI experiment showed little difference in binding to probes N1 and N1c. However, menin was preferentially enriched by probe N1 (Fig. 2, B and C),

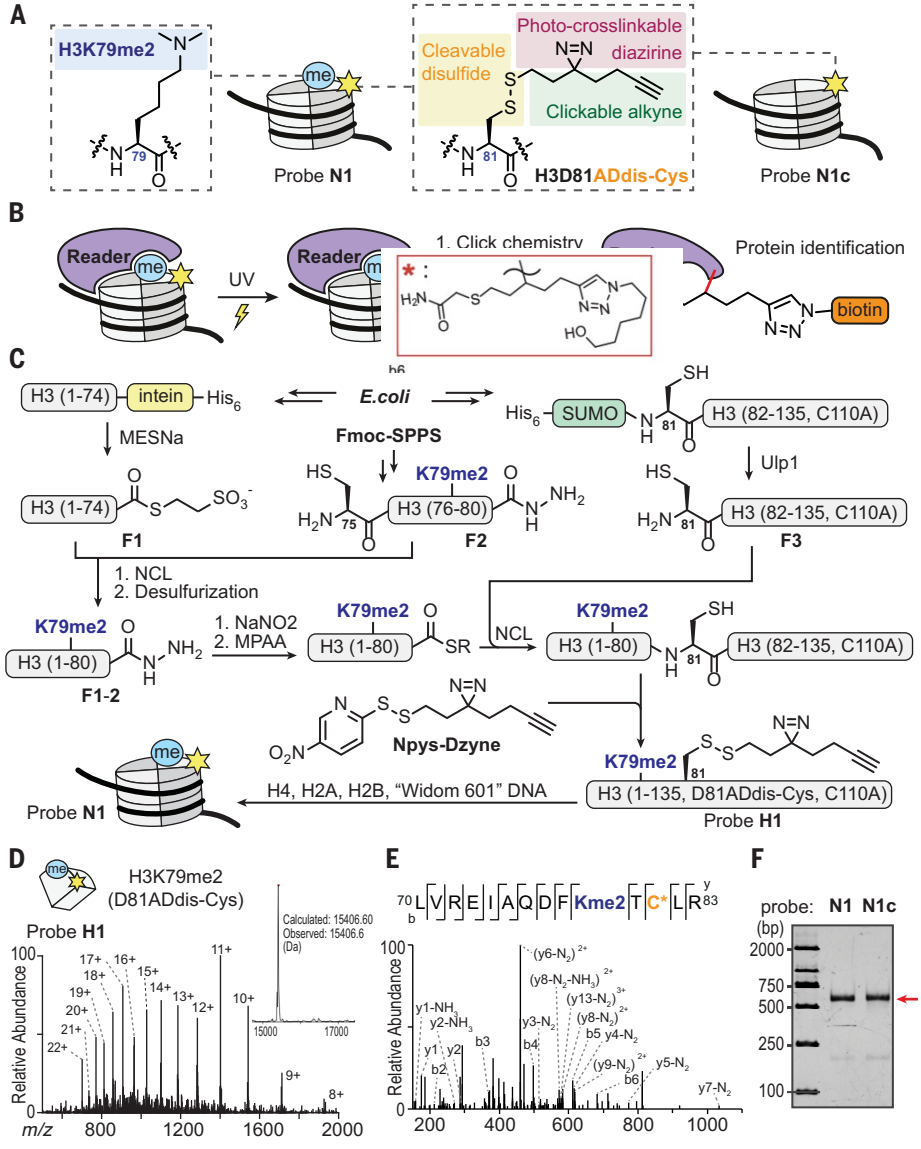

Fig. 1. Development of nucleosome-based photoaffinity probes. (**A**) Illustration and partial structure of probes N1 and N1c. (**B**) Workflow for H3K79me2 "reader" identification using probe N1. (**C**) Synthetic route to generating histone H3K79me2 (D81ADdis-Cys, C110A) (probe H1). (**D**) ESI-MS analysis of probe H1. (**E**) A representative MS/MS spectrum of probe H1, ^{70}LVREIAQDF Kme2 T ADdis-Cys LR^{83}. C*, ADdis-Cys. (**F**) The quality of purified nucleosome probes N1 and N1c examined by native polyacrylamide gel electrophoresis. The gel was stained by ethidium bromide. Red arrow, reconstituted nucleosome probes. Single-letter abbreviations for the amino acid residues are as follows: A, Ala; C, Cys; D, Asp; E, Glu; F, Phe; G, Gly; H, His; I, Ile; K, Lys; L, Leu; M, Met; N, Asn; P, Pro; Q, Gln; R, Arg; S, Ser; T, Thr; V, Val; W, Trp; and Y, Tyr.

suggesting that it may recognize the H3K79me2 mark on the nucleosome. The selective capture and enrichment of endogenous menin by the methylated nucleosome probe N1 was confirmed by the immunoblotting analysis (Fig. 2D).

Menin is associated with H3K79me2 nucleosomes in cells

To further validate the interaction between menin and the H3K79me2 nucleosome in cells, we overexpressed FLAG-tagged menin in human embryonic kidney 293T (HEK293T) cells and examined whether it could act as a "bait" to pull down nucleosomes in an H3K79 methylation-dependent manner. We isolated nuclei from the cells and treated them with micrococcal nuclease (MNase) to generate the mononucleosomes, which were then subjected to immunoprecipitation using anti-FLAG M2 magnetic beads (fig. S2A). The immunoblotting analysis using the anti-H3 antibody revealed that the mononucleosomes were indeed enriched by FLAG-menin, confirming the association of menin with the nucleosome. The amount of mononucleosomes enriched by FLAG-menin decreased after cells were treated with EPZ5676, a DOT1L inhibitor (*22*) that reduces cellular H3K79me2 level. By contrast, more nucleosomes were enriched by FLAG-menin when the H3K79me2 level was increased by overexpressing DOT1L in the cells (fig. S2B). These results indicate that the interaction between menin and the nucleosome is likely mediated by H3K79 dimethylation.

Menin selectively binds to H3K79me2 nucleosomes in vitro

We next examined whether menin could directly and selectively bind to H3K79me2 nucleosome. To this end, a photocrosslinking experiment was performed with the recombinant menin protein in vitro. As expected, probe N1 captured menin more efficiently than probe N1c (Fig. 2E), validating the methylation-dependent association of menin to the nucleosome. Menin was robustly captured by the nucleosome-based probe N1 but was not captured by the H3 protein-only probe H1 (fig. S2C), indicating that the binding of menin to H3K79me2 requires an intact nucleosome. The selective binding of menin to H3K79me2 nucleosome was also confirmed by nucleosome-based probes N2 and N2c without photoaffinity handles (Fig. 2F and fig. S2, D and E). To determine whether menin formed a stable complex with the H3K79me2 nucleosome, we performed an electrophoretic mobility shift assay (EMSA) using H3K79me2 nucleosome probe N3, which contains Cy5-labeled DNA (Fig. 2G and fig. S2, F and G). We observed a new band with lower mobility, indicating the formation of a stable menin-nucleosome complex with probe N3. The dissociation constant was estimated to be ~6.4 μM (Fig. 2H).

Structural overview of menin bound to H3K79me2 nucleosome

To understand the molecular basis for how menin recognizes the H3K79me2 mark on nucleosome, we reconstituted the menin-H3K79me2 nucleosome complex (hereafter "Menin-H3K79me2") (fig. S3, A to C), crosslinked by GraFix (*23*), for structure determination using cryo–electron microscopy (cryo-EM). We obtained an H3K79me2 nucleosome structure at 2.9-Å resolution and a Menin-H3K79me2 nucleosome structure at ~3.2-Å resolution (fig. S3, D to O). In the Menin-H3K79me2 structure, menin binds to only one face of the nucleosome disk (fig. S3D and movie S1), covering almost half of the nucleosome face (Fig. 3, A to D) and adopting a conformation similar to that of a previous crystal structure of menin (*24*).

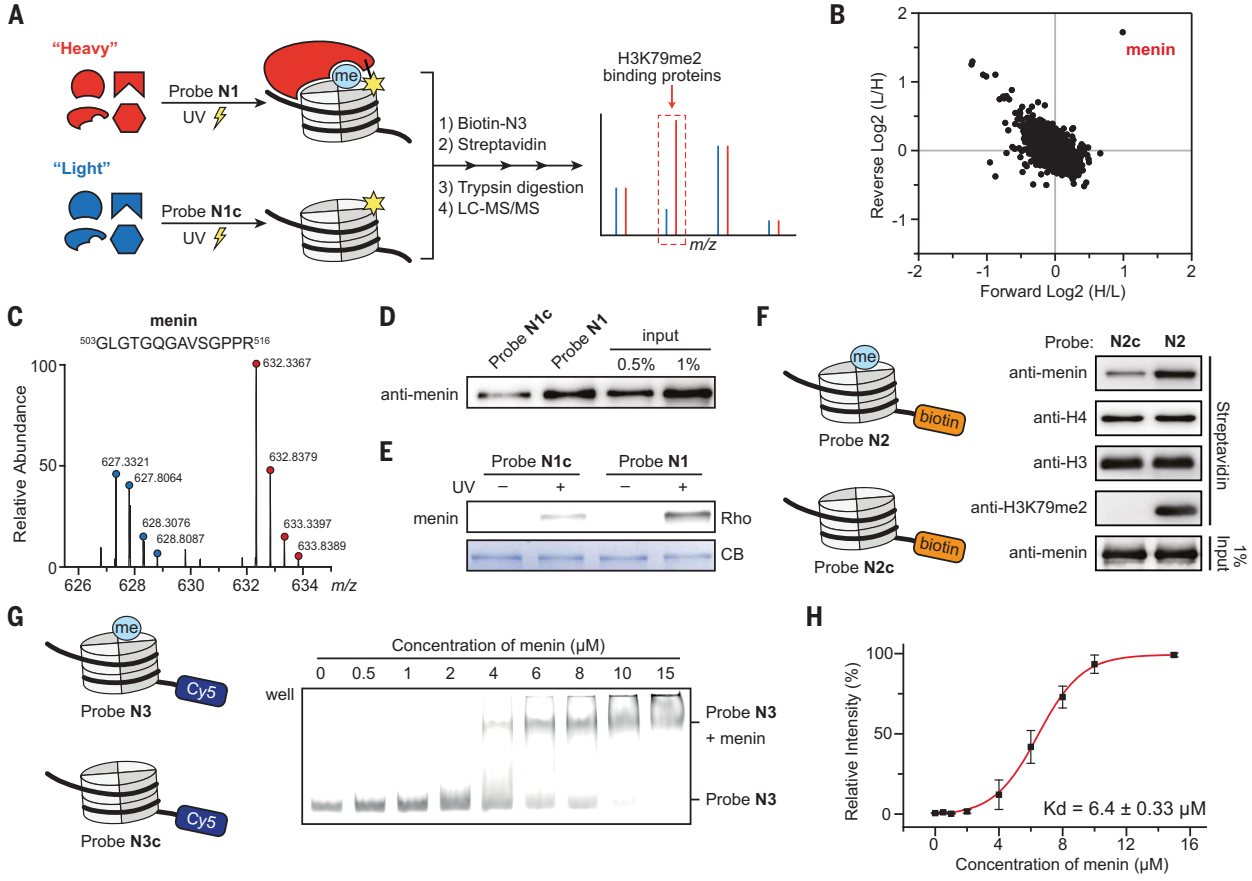

Fig. 2. Identification of menin as an H3K79me2-binding protein in a nucleosomal context. (**A**) Workflow of the CLASPI approach to identify H3K79me2 binders. (**B**) Two-dimensional plot showing that menin stands out from the forward and reverse CLASPI experiments. Data from table S1 are used. (**C**) A representative MS1 spectrum from menin in CLASPI experiments. (**D**) Pull-down of menin by probes N1 and N1c in nuclear extract. (**E**) Photocrosslinking assay of recombinant menin by probes N1 and N1c. Rho, rhodamine fluorescence signal; CB, Coomassie blue staining. (**F**) Non-crosslinking pull-down revealed interaction between menin and nucleosomes. (**G**) EMSA result of Cy5-labeled H3K79me2 nucleosome probe N3 titrated with menin. (**H**) Measurement for the binding affinity of menin toward the H3K79me2 nucleosome in the EMSA assay. Relative intensities of the complex band were plotted against the concentration of menin. Error bars represent mean ± SE (n = 3 biological replicates).

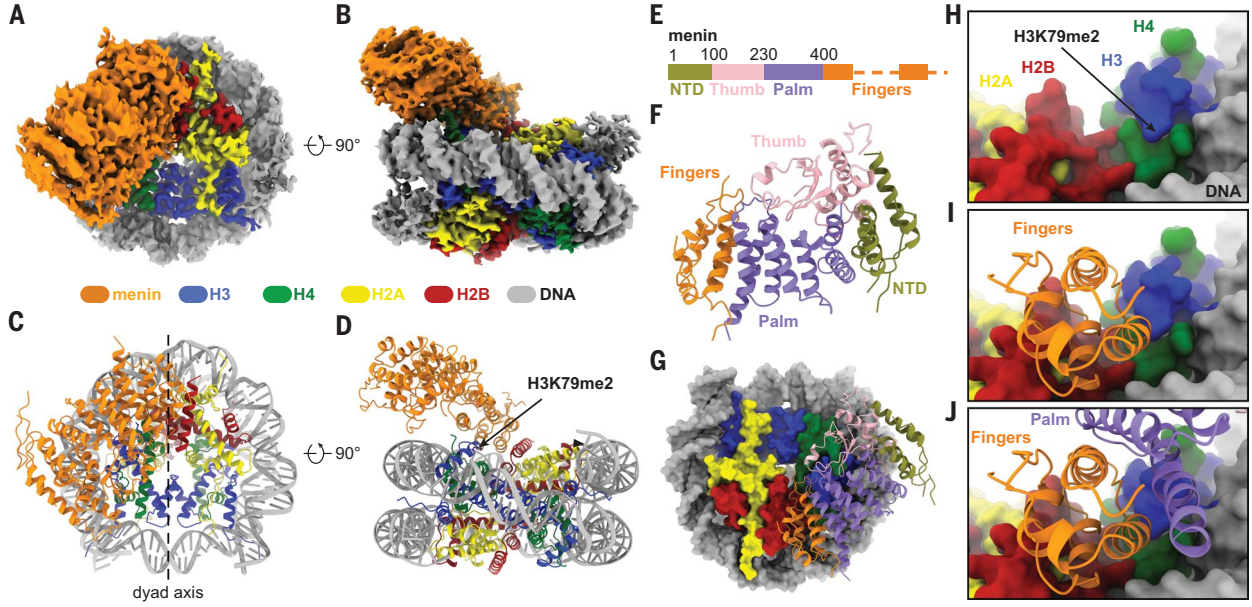

Fig. 3. Overall structure of menin-H3K79me2 nucleosome complex. (**A** and **B**) Top (A) and side (B) views of the segmented cryo-EM map of menin-H3K79me2 nucleosome complex. (**C** and **D**) Same as (A) and (B), respectively, but shown with the atomic model. (**E**) Schematic domain organization of menin. (**F**) Overview of the nucleosome-bound menin structure shown in a cartoon view. The different domains are colored as indicated. (**G** to **J**) H3K79me2 recognition mediated by the fingers and palm domains of menin.

H433 of menin is a key residue for the recognition of H3K79me2 via a π-cation interaction

Menin binds to H3K79me2 nucleosome through its fingers and palm domains (Fig. 3, E to J). The fingers domain engages with the C-terminal α helix of H2B (H2B αC) mainly through three hydrogen bonds on top of the four-helix bundle between H2B and H4 (Fig. 4, A and B, and fig. S3P). This docking is further reinforced by the palm domain through its C-terminal long helix forming four hydrogen bonds with the H3 L1 loop and α1 helix (Fig. 4, C and D, and fig. S3Q). These interactions together place menin in a position to capture the side chain of

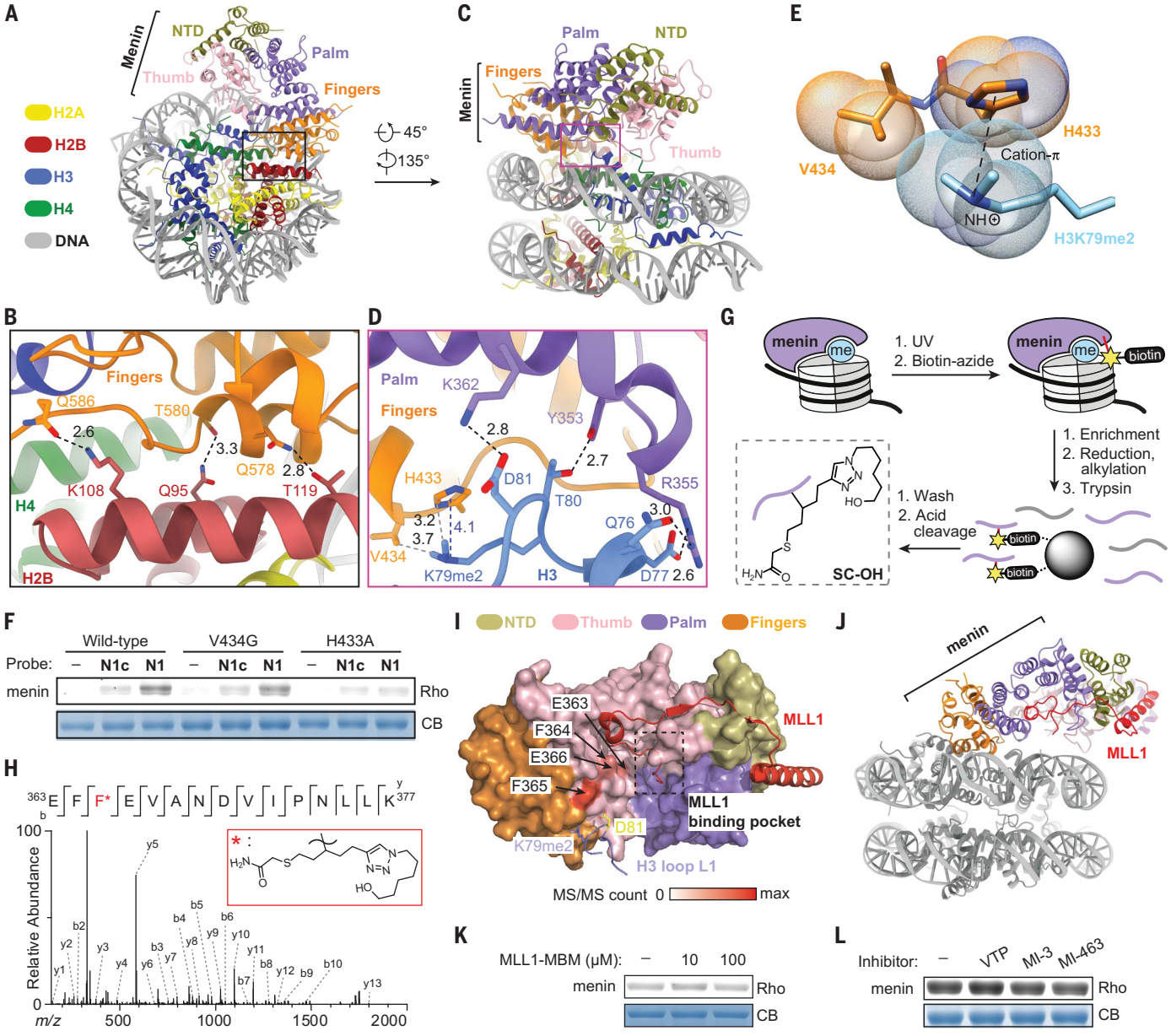

Fig. 4. Menin "reads" H3K79me2 through a π-cation interaction with H433 from its fingers domain. (**A** and **B**) The fingers domain of menin engages with the C-terminal α helix of H2B. Magnified view of the boxed region highlights the interaction details. The hydrogen bonds are indicated by dashed lines. Interatomic distances are shown in angstroms. (**C** and **D**) Menin's palm domain interacts with H3 L1 loop through forming four hydrogen bonds, while H433 from its fingers domain recognizes H3K79me2 through π-cation interaction. (**E**) Magnified view of the π-cation interaction between menin H433 and H3K79me2. The side chains of H433 and V434 and the methylammonium moieties of H3K79me2 are highlighted by the dotted van der Waals radius representation. (**F**) Photocrosslinking assay of recombinant wild-type, V434G, and H433A menin by probe N1 and N1c. Rho, rhodamine fluorescence signal; CB, Coomassie blue staining. (**G**) The workflow used to map the H3K79me2-binding sites of menin. (**H**) A representative MS/MS spectrum for identified SC-OH–labeled menin peptide, ^{363}EFF(SC-OH)EVANDVIPNLLK^{377}. (**I**) Mapping of the identified H3K79me2-binding sites of menin to our structure in surface representation. H3 Loop L1 is shown in cartoon view except that H3K79me2 and H3D81 (where the photocrosslinker is incorporated) are shown in stick format. The heatmap is generated based on the MS/MS counts of "SC-OH" labeled residues (data from table S2). MLL1 from the crystal structure of menin-MLL1-LEDGF (PDB: 3U88), superimposed with our structure, shown in cartoon view. (**J**) Superimposition of the structures of menin-H3K79me2 nucleosome and menin-MLL1-LEDGF (PDB: 3U88) using menin as a reference. (**K** and **L**) Photocrosslinking assay of menin by probe N1 in the presence of MLL1-MBM (K) or menin-MLL1 inhibitors (L).

the H3K79me2 (Figs. 3 and 4). It thus stabilizes the methylammonium moieties of H3K79me2 by both π-cation and hydrophobic interactions with H433 and V434 from its fingers domain (Fig. 4, D and E). Of note, menin binding does not induce obvious conformational changes in histones (fig. S4). Consistent with this observation, the H3K79me2 nucleosome probe N1 showed a largely reduced cross-linking efficiency toward a menin H433A mutant, when compared with the wild-type (Fig. 4F). The unmodified nucleosome probe N1c, which captured menin at much lower efficiency (Fig. 2E), showed little preference for capturing the wild-type or the mutated menin (Fig. 4F). Mutation of V434 to glycine, however, did not affect the binding, suggesting that the hydrophobic interaction mediated by V434 is not essential for H3K79me2 recognition (Fig. 4F). Together, these data demonstrate the key role of H433 of menin in the recognition of the H3K79me2 mark on nucleosome. Our attempt to assemble menin onto the unmodified nucleosome for structural determination was unsuccessful

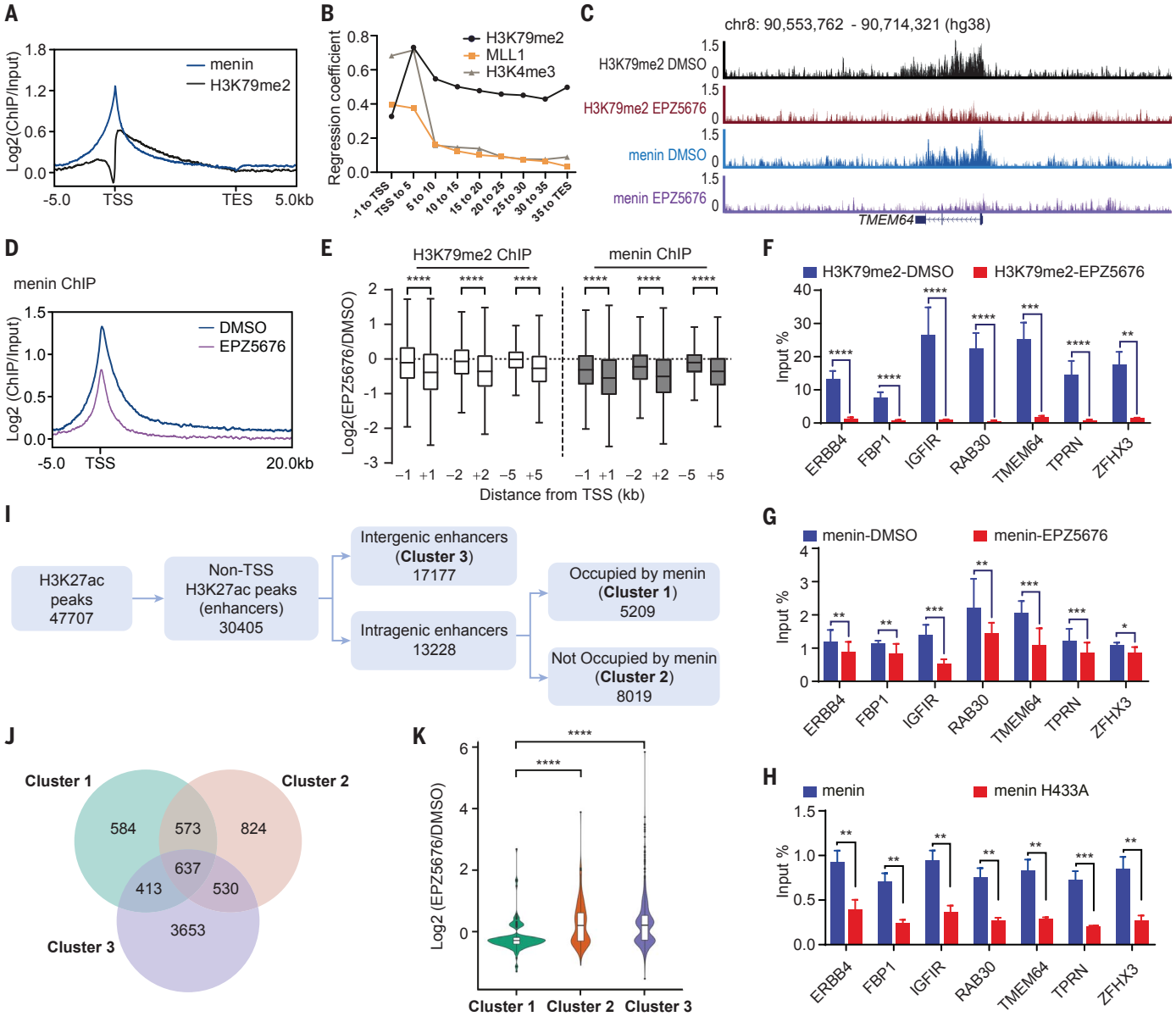

Fig. 5. Menin colocalizes with H3K79me2 at intragenic enhancers and regulates gene transcription. (**A**) Menin and H3K79me2 $\log_2$(ChIP-seq/Input) signal across the gene body. (**B**) Linear regression coefficient of H3K79me2, H3K4me3, and MLL1 ChIP-seq signal/input against MEN1 ChIP-seq/input from the promoter (−1 kb to TSS) through the gene body. (**C**) ChIP-seq signal of H3K79me2 and menin with dimethyl sulfoxide (DMSO) and EPZ5676 treatment at the *TMEM64* locus. (**D**) Menin $\log_2$(ChIP-seq/Input) signal with (EPZ5676) and without (DMSO) Dot1L inhibitor treatment across the gene body. (**E**) Box plot illustrating average $\log_2$(EPZ5676/DMSO) signal over 1, 2, and 5 kb upstream and downstream regions from the TSS. (**F** and **G**) ChIP-qPCR analyses showing the changes in chromatin loci of H3K79me2 (F) and menin (G) on the indicated intragenic regions upon EPZ5676 treatment (n = 6 biological replicates). (**H**) ChIP-qPCR analyses of cells stably expressing wild-type menin or menin H433A on the indicated intragenic regions (n = 6 biological replicates). (**I**) Schematic diagram illustrating how different categories of enhancers are defined. (**J**) Venn diagram showing overlap of genes associated with enhancers from different clusters. (**K**) Violin plot of RNA-seq data representing differential gene expression [$\log_2$(EPZ5676/DMSO)] with specific genes from each cluster (****P < 0.0001). Only significantly differentially expressed genes (adjusted P value < 0.05) are included. Error bars indicate ±SE.*P < 0.05, **P < 0.01, ***P < 0.001, ****P < 0.0001.

(fig. S3, R and S), likely owing to a largely reduced stability of the menin-nucleosome complex in the absence of H3K79 methylation. Unlike readers of lysine methylation on histone tails, which often capture the methylammonium moiety using an "aromatic cage" constituted with two to four aromatic residues (*25*), menin recognizes H3K79me2 by π-cation interaction with only one aromatic residue, H433. This binding is likely further enhanced by the extensive interactions of menin with histones H3 and H2B of the nucleosome to confer a specific H3K79me2 recognition in a nucleosomal context.

Menin binds H3K79me2 nucleosome and MLL using two different pockets

To provide another line of structural information, we mapped the binding site of menin using our photocrosslinking strategy (*26*). The trifunctional handle of probe N1 enabled crosslinking of the H3K79me2-binding region of menin for enrichment and allowed the release of the cross-linked fragment for MS analysis (Fig. 4G). Notably, only one peptide containing four putative cross-linked residues (E363, F364, F365, E366) was identified in the MS analysis (Fig. 4H), indicating that the binding was highly specific. We mapped these cross-linked residues onto the cryo-EM structure of menin-H3K79me2 nucleosome. The cross-linked residue with the highest MS/MS count, F365, was indeed close to the H3D81 position where the photoreactive warhead was installed (fig. S5, A to C). Considering that the photocrosslinking reaction is highly sensitive to distance, the in-solution structural features of menin at its H3K79me2-binding pocket revealed by the photocrosslinking assay agree well with the solved cryo-EM structure. Of note, the binding sites were located at the boundary between the palm domain and the fingers domain but distal to a conserved binding pocket of several known menin-interacting proteins such as mixed lineage leukemia protein–1 (MLL1) (*24*) (Fig. 4I).

In addition, we also performed a structural comparison between the crystal structure of menin-MLL1-LEDGF (PDB: 3U88) (*24*) and our menin-H3K79me2 nucleosome structure. From Fig. 4J and fig. S5, D to I, it is apparent that the overall architectures of menin from these two structures are similar, suggesting that nucleosome binding does not cause a major conformational change in menin. Whereas menin is recruited onto the H3K79me2 nucleosome via its fingers and palm domains, MLL1-LEDGF mainly associates with the palm and NTD domains. MLL1 embeds its N-terminal menin-binding motif (MBM) deeply into the peptide binding pocket of the palm domain of menin, further extending its remaining part onto the surface of the NTD domain to reach LEDGF on the side far away from the site for nucleosome binding. This structural analysis suggests that menin is capable of binding to both nucleosome and MLL1-LEDGF at the same time without steric clash. Indeed, MBM of MLL1 (^{6}RWRFPARPGTTGGGGGGGRR^{25}) and known menin-MLL1 inhibitors (VTP50469, MI-3, and MI-463) (*27*–*29*) did not abolish the menin-H3K79me2 nucleosome interaction in our photocrosslinking experiment (Fig. 4, K and L). Additionally, the interaction between menin and MLL1 was also not affected by mutating menin's H3K79me2-recognition residue (H433A) (fig S5, J and K), corroborating that menin has two independent binding pockets for MLL1 and H3K79me2 nucleosome. Together, these results suggest that the NTD and palm domains of menin might be important for recruiting menin's associating factors such as JunD or MLL1 to chromatin (*24*).

Menin is associated with H3K79me2 across gene bodies

To examine whether menin recognizes the H3K79me2 mark on native chromatin, we performed chromatin immunoprecipitation sequencing (ChIP-seq) in MCF-7 cells. Consistent with previous studies (*30*, *31*), the H3K79me2 mark was found to peak immediately downstream of the transcription start site (TSS), and the signal diminished throughout the gene body (Fig. 5A and fig. S6A). Menin was previously reported to associate with MLL1 and thereby localize at promoter regions (*27*, *32*). Indeed, menin occupied the promoters and peaked at the TSSs of many active genes in our analysis (Fig. 5A and fig. S6A). However, regression analysis showed that correlation between menin and MLL1–H3K4me3 was only observed around the TSSs. By contrast, the menin signal was strongly predictable by H3K79me2 across the gene body (Fig. 5B).

To further investigate the effects of H3K79me2 on the binding of menin to chromatin, we treated cells with EPZ5676, a DOT1L inhibitor, which resulted in a near-complete global loss of H3K79me2 as detected by immunoblotting (fig. S6, B and C) and by reference-normalized ChIP-seq (Fig. 5C and fig. S6D). The loss of H3K79me2 had no effect on the expression of menin (fig. S6, B and C), but attenuated the interaction between menin and chromatin (Fig. 5, C and D). Consistently, menin binding downstream of TSSs was more sensitive to EPZ5676 treatment compared with menin peaks in the promoter region upstream of the TSS (Fig. 5E). ChIP-qPCR (quantitative polymerase chain reaction) confirmed that the loss of H3K79me2 strongly interfered with the recruitment of menin to the gene bodies of target genes (Fig. 5, F and G), and modestly affected the genomic localization of menin at the promoters (fig. S6, E and F). To further validate that the identified menin binding sites were H3K79me2 dependent, we performed ChIP-qPCR with cells stably expressing either the hemagglutinin (HA)–tagged wild-type menin or the equivalent H433A mutant (fig. S6G). In line with our in vitro biochemical data, the H433A mutation largely disrupted menin's association with chromatin at the selected intragenic regions (Fig. 5H).

Menin is involved in transcriptional regulation through binding to H3K79me2 at potential intragenic enhancers

It was previously proposed that H3K79me2 could activate the expression of target genes through the maintenance of enhancer–promoter interactions (*30*, *33*). Given the correlation between menin and H3K79me2 at genic regions, we explored whether the H3K79me2-menin interaction could mark functional enhancers. To this end, we identified putative enhancers from the presence of H3K27ac peaks (*34*, *35*), then classified them as intragenic or intergenic. We further subcategorized the intragenic enhancers into two groups on the basis of menin occupancy (Fig. 5I and fig. S7A). We correlated these enhancers to their overlapping gene or closest gene based on genomic distance (Fig. 5J). As many genes were regulated by multiple enhancers in each group, we focused on genes that were specifically associated with each type of enhancer: intragenic MEN1-bound (cluster 1), intragenic MEN1-free (cluster 2), and intergenic (cluster 3) (table S3). Most cluster 1 regions overlapped with cis-regulatory regions annotated by ENCODE (Encyclopedia of DNA Elements), and some also show evidence of expression of enhancer RNA (fig. S7B). On the basis of differential expression, we found that EPZ5676 treatment led to significant down-regulation of genes in cluster 1 containing menin-marked enhancers compared with the other clusters, as well as randomly selected gene sets with matched expression levels in untreated cells (Fig. 5K and fig. S7, C to E). Consistent with the transcriptome analysis, EPZ5676 treatment significantly blocked the expression of genes in cluster 1 (fig. S7F). Overall, these data render the possibility that menin might recognize the H3K79me2 mark at intragenic enhancers to mediate gene transcription.

In this study, we identified menin as a bona fide reader of H3K79me2. Menin is known to be involved in transcriptional regulation by interacting with various transcription factors and chromatin regulatory proteins (*36*–*39*). Our study therefore adds a mechanistic possibility that menin recruits its interacting proteins to H3K79me2-marked chromatin regions for gene regulation. Considering that MLL1 is a histone H3K4 methyltransferase, we envision that future studies will reveal whether and how menin may mediate cross-talk between H3K4me3 and H3K79me2 on gene regulation.

REFERENCES AND NOTES

1. E. L. Greer, Y. Shi, *Nat. Rev. Genet.* **13**, 343–357 (2012).
2. A. Jambhekar, A. Dhall, Y. Shi, *Nat. Rev. Mol. Cell Biol.* **20**, 625–641 (2019).
3. K. Hyun, J. Jeon, K. Park, J. Kim, *Exp. Mol. Med.* **49**, e324 (2017).
4. Y. Huyen *et al*., *Nature* **432**, 406–411 (2004).
5. R. Alpatov *et al*., *Cell* **157**, 869–881 (2014).
6. H. Wu *et al*., *PLOS ONE* **6**, e18919 (2011).
7. M. Sabra, P. Texier, J. El Maalouf, P. Lomonte, *J. Cell Sci.* **126**, 3664–3677 (2013).
8. Q. Feng *et al*., *Curr. Biol.* **12**, 1052–1058 (2002).
9. F. van Leeuwen, P. R. Gafken, D. E. Gottschling, *Cell* **109**, 745–756 (2002).
10. K. Wood, M. Tellier, S. Murphy, *Biomolecules* **8**, 11 (2018).
11. B. Zhu *et al*., *Nat. Commun.* **9**, 259 (2018).
12. T. P. Wakeman, Q. Wang, J. Feng, X. F. Wang, *EMBO J.* **31**, 2169–2181 (2012).
13. W. Kim, M. Choi, J. E. Kim, *Cell Cycle* **13**, 726–738 (2014).
14. E. R. Barry *et al*., *Stem Cells* **27**, 1538–1547 (2009).
15. Y. Feng *et al*., *Blood* **116**, 4483–4491 (2010).
16. B. Jones *et al*., *PLOS Genet.* **4**, e1000190 (2008).
17. K. M. Bernt *et al*., *Cancer Cell* **20**, 66–78 (2011).
18. X. Lu *et al*., *Nat. Struct. Mol. Biol.* **15**, 1122–1124 (2008).
19. T. W. Muir, D. Sondhi, P. A. Cole, *Proc. Natl. Acad. Sci. U.S.A.* **95**, 6705–6710 (1998).
20. J. S. Zheng, S. Tang, Y. K. Qi, Z. P. Wang, L. Liu, *Nat. Protoc.* **8**, 2483–2495 (2013).
21. X. Li *et al*., *J. Am. Chem. Soc.* **134**, 1982–1985 (2012).
22. S. R. Daigle *et al*., *Blood* **122**, 1017–1025 (2013).
23. B. Kastner *et al*., *Nat. Methods* **5**, 53–55 (2008).
24. J. Huang *et al*., *Nature* **482**, 542–546 (2012).
25. S. D. Taverna, H. Li, A. J. Ruthenburg, C. D. Allis, D. J. Patel, *Nat. Struct. Mol. Biol.* **14**, 1025–1040 (2007).
26. J. Lin, X. Bao, X. D. Li, *Mol. Cell* **81**, 2669–2681.e9 (2021).
27. A. V. Krivtsov *et al*., *Cancer Cell* **36**, 660–673.e11 (2019).
28. J. Grembecka *et al*., *Nat. Chem. Biol.* **8**, 277–284 (2012).
29. D. Borkin *et al*., *Cancer Cell* **27**, 589–602 (2015).
30. L. Godfrey *et al*., *Nat. Commun.* **10**, 2803 (2019).
31. G. Nassa *et al*., *Sci. Adv.* **5**, eaav5590 (2019).
32. K. M. A. Dreijerink *et al*., *Cell Rep.* **18**, 2359–2372 (2017).
33. L. Godfrey *et al*., *Leukemia* **35**, 90–106 (2021).
34. N. D. Heintzman *et al*., *Nat. Genet.* **39**, 311–318 (2007).
35. N. D. Heintzman *et al*., *Nature* **459**, 108–112 (2009).
36. A. Yokoyama *et al*., *Cell* **123**, 207–218 (2005).
37. S. K. Agarwal *et al*., *Cell* **96**, 143–152 (1999).
38. S. Jin *et al*., *J. Clin. Invest.* **120**, 593–606 (2010).
39. H. Sowa *et al*., *J. Biol. Chem.* **279**, 40267–40275 (2004).

ACKNOWLEDGMENTS

Funding: This work was supported by funds from the Hong Kong Research Grants Council Areas of Excellence Scheme (AoE/P-705/16 to X.D.L.); Collaborative Research Fund (CRF C7028-19G to X.D.L., CRF C7009-20G to Y.Z.) and the General Research Fund (GRF 17121120, 17310122 to X.D.L.); Excellent Young Scientists Fund of China (Hong Kong and Macau) (21922708 to X.D.L.); Science and Technology Innovation Committee of Shenzhen (SGDX20201103095201O1 to X.D.L.); Centre for Oncology and Immunology under the Health@InnoHK Initiative funded by the Innovation and Technology Commission, the Government of Hong Kong SAR, China (J.W.H.W); and the K. C. Wong Educational Foundation (GJTD-2020-06). The EM dataset was collected at the Biological Cryo-EM Center, generously supported by a donation from the Lo Kwee Seong Foundation, at HKUST. Cryo-EM data processing was performed in workstations and the cluster HPC3 supported by the Information Technology Services Center (ITSC) at HKUST. We thank Y. Zhang (Biological Cryo-EM Center, HKUST) and P. W. Luo (ITSC, HKUST) for their support. D.Y. is supported by an LKS fellowship. **Author contributions:** Design of experiments: X.D.L., J.L., Y.W., X.B., and G.T. Probe synthesis: Y.W., J.L., Y.J., and Z.L. Mass spectrometry sample preparation and data analysis: Y.W., X.B., and J.L. Validation of H3K79me2-menin interaction in vitro and in cells: J.L., Y.W., and G.T. Cryo-EM sample preparation: J.L., W.L., D.Y., Y.Z., and S.D. Cryo-EM data analysis: D.Y., W.L., Y.Z., and S.D. ChIP-seq and RNA-seq sample preparation: X.B. and G.T. ChIP-seq and RNA-seq data analysis: J.W.H.W. and E.Y. Writing – original draft: Y.W., Y.Z., X.B., and G.T. Writing – review and editing: X.D.L., Y.Z., J.W.H.W., X.B., and J.L. Visualization: J.L., Y.Z., Y.W., D.Y., J.W.H.W., E.Y., X.B., and G.T. **Competing interests:** The authors declare that they have no competing interests. **Data and materials availability:** The menin-H3K79me2 nucleosome cryo-EM model and map reported in this paper have been deposited in the Protein Data Bank (PDB) and Electron Microscopy Data Bank (EMDB), respectively, with accession numbers 8GPN (PDB) and EMD-34195 (EMDB). The raw sequencing data for ChIP-seq and RNA-seq analyses presented in this paper have been deposited in Gene Expression Omnibus with the accession number GSE202593. All other data are available in the main text or the supplementary materials. Newly created materials from this study may be requested from the corresponding authors.

SUPPLEMENTARY MATERIALS

science.org/doi/10.1126/science.adc9318
Materials and Methods
Figs. S1 to S7
Tables S1 to S5
Data S1 and S2
References (*40*–*58*)
MDAR Reproducibility Checklist
Movie S1

View/request a protocol for this paper from *Bio-protocol*.

Submitted 10 May 2022; resubmitted 29 August 2022
Accepted 5 January 2023
10.1126/science.adc9318

Menin “reads” H3K79me2 mark in a nucleosomal context

Jianwei Lin, Yiping Wu, Gaofei Tian, Daqi Yu, Eunjeong Yang, Wai Hei Lam, Zheng Liu, Yihang Jing, Shangyu Dang, Xiucong Bao, Jason Wing Hon Wong, Yuanliang Zhai, and Xiang David Li

Science **379** (6633), . DOI: 10.1126/science.adc9318

A reader for H3K79me2

Decoding a histone modification requires identification of proteins that “read” the mark. Methylation of histone H3 lysine-79 (H3K79) plays key roles in gene regulation, but it remains a mystery how this histone mark is recognized and interpreted by specific readers. Lin *et al*. identified the protein menin as a bona fide reader of H3K79me2 using a multifunctional nucleosome-based photoaffinity probe. Biochemical and structural studies using cryo–electron microscopy revealed that menin engages with the H3K79me2 nucleosome through multivalent contacts. —DJ